International Communications in Heat and Mass Transfer 37 (2010) 1072–1077

Contents lists available at ScienceDirect

International Communications in Heat and Mass Transfer

journal homepage: www.elsevier.com/locate/ichmt

Computations of shear driven vortex flow in a cylindrical cavity using a modified k-ε turbulence model ☆

Khalid M. Saqr [a,*], Hossam S. Aly [b], Hassan I. Kassem [a], Mohsin M. Sies [a], Mazlan A. Wahid [a]

[a] High-Speed Reacting Flow Laboratory, Faculty of Mechanical Engineering, Universiti Teknologi Malaysia, 81310 Skudai, Johor Bahru, Malaysia
[b] Department of Aeronautical Engineering, Faculty of Mechanical Engineering, Universiti Teknologi Malaysia, 81310 Skudai, Johor Bahru, Malaysia

ARTICLE INFO

Available online 6 July 2010

Keywords:
Shear driven cavity flow
Lid-driven cavity
Turbulence modeling
Vortex flow
Flow in open cylindrical cavities

ABSTRACT

In this paper, a new variant of the k-ε turbulence model (Saqr et al., CFD Letters, 1(2) pp. 87–94) is used to compute the shear driven vortex flow in an open cylindrical cavity. The results are compared with published LDA measurements for such flow configuration. The modified turbulence model demonstrated good agreement with experimental results, which further supports its validity in computing vortex dominated flows.

1. Introduction

The shear driven cavity flow is one of the classical fluid dynamics problems that can narrate the development of modern understanding of fluid dynamics. Literature records include research on such problem since 1965 [1] until today [2,3]. The shear-driven cavity flow has been extensively used to validate new numerical schemes [4–6] and new turbulence models [7–9]. In addition, the shear-driven flow physics has been of notable importance to several engineering applications [10–12]. The vast majority of these researches have considered cavities with rectangular cross section, with different aspect ratios. The shear-induced cavity flow is generally characterized by dominated vortices in the turbulent flow regime [13–16]. Bruneau and Saad [17] have recently conducted remarkable effort to thoroughly describe the vortex behavior in square lid-driven cavity flows at a wide range of Reynolds numbers. In addition to providing accurate benchmark data for the problem, they reported comprehensive data on the formation of the primary and secondary vortices.

When the shear-driven flow is enclosed in a circular cavity, it exhibits unrelenting behavior of circulation and vortical motion. Mercan and Atalik [18] have reported such phenomenon in arc-shaped cavities at numerous high Reynolds numbers. Recently, the shear driven flow inside a cylindrical cavity was experimentally studied by Savelsberg and Castro [19]. Their work complimented few researches on the shear-driven flow in semi-cylindrical cavities, such as [10,16,20]. The findings of these researches commonly described the formation and sustenance of a dominating vortex, with a solid-body rotating core in the shear induced flow in circular cavities. However, the contemporary literature reveals that the problem of shear-driven flow inside cylindrical or semi-cylindrical cavities has attracted far less attention than such of flow inside square or rectangular cavities.

The present work describes the results of several numerical computations, using a new variant of the standard k-ε, of the turbulent shear driven vortex flow in an open cylinder cavity. The work relies on the LDA measurements published by Savelsberg and Castro [19] to provide a comparative benchmark for the modified turbulence model that has been recently proposed and validated by the authors for vortex dominated flows [21].

2. Flow configuration

Fig. 1 shows a schematic of the actual flow configuration according to [19]. Air was supplied to the flow domain at different inlet velocities ranging from 5.9 m/s to 14.03 m/s. The opening angle of the cavity (named ϕ) was set to four different values, viz. 20°, 40°, 60° and 80°. In the present analysis, the computations are conducted on a two dimensional plane parallel to the XZ plane, as in Fig. 1b. This two dimensional approximation was undertaken based on a physical assumption that the circumferential behavior of the shear driven vortex is relatively unaffected by the three dimensionality of the flow. Point (B) is the where the main flow separates in the 2D case considered in the present study. The opening angle was set to 40° in all computations. Readers are advised to refer to the comprehensive analysis of Savelsberg and Castro [19] for further details on the assembly of the experimental rig and the Laser Doppler Anemometry (LDA) measurement procedures.

☆ Communicated by W.J. Minkowycz.

* Corresponding author.
E-mail addresses: khaledsaqr@gmail.com, mmdmskhalid2@live.utm.my (K.M. Saqr).

0735-1933/$ – see front matter © 2010 Elsevier Ltd. All rights reserved.
doi:10.1016/j.icheatmasstransfer.2010.06.021

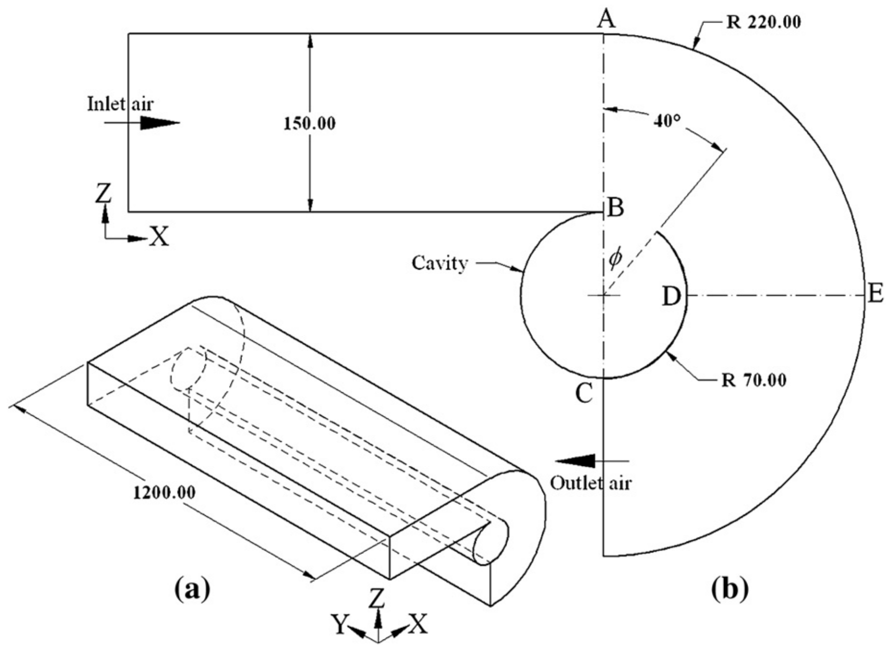

Fig. 1. Flow configuration in the open cylinder cavity after [19]. Dimensions in mm. (a) a schematic of the 3D flow configuration and (b) the 2D flow domain considered in the present study.

3. Governing equations

3.1. Conservation of mass and momentum

The Reynolds-averaged equations of motion, in tensor notation, for the steady-state two dimensional flow are [22]:

$$\text{Conservation of mass}: \ \frac{\partial U_i}{\partial x_i} = 0 \tag{1}$$

$$\text{Conservation of momentum}: \rho \frac{\partial}{\partial x_j}\left(U_j U_i + \overline{u_j' u_i'}\right) = -\frac{\partial P}{\partial x_i} + \frac{\partial}{\partial x_j}\left(2\mu S_{ij}\right) \tag{2}$$

where U_i is the mean velocity, x_i is the position vector, $\overline{u_j' u_i'}$ is the temporal average of fluctuating velocity, P is the mean static pressure, μ is the molecular viscosity and S_{ij} is the strain rate expressed as $\frac{1}{2}\left(\frac{\partial u_i}{\partial x_j} + \frac{\partial u_j}{\partial x_i}\right)$.

The local air density was calculated based on a fixed value for the operating pressure, which equals to the ambient pressure. In other words, the air flow was assumed to be incompressible. This assumption was made after ensuring the inlet Mach number is particularly less than 0.3 in all cases [23].

3.2. The R_ε/k-ε turbulence model

In fact, the standard *k*-ε model has been reported to provide good predictions of vortex/swirl dominated flows, such as in swirl combustors [24–33] and hydrocyclones [34], despite all the theoretical objections on its performance in such cases. However, several attempts have been carried out to enhance the predictability of the standard *k*-ε model with vortex dominated flows. These attempts have been recently reviewed by the authors in [21]. One modification that has been reported to yield satisfactory results in vortex flows is the RNG/*k*-ε model. The model was presented by Yakhot and Orszag based on the application of the Renormalization group (RNG) theory [35,36]. They have used a sophisticated scale elimination procedure to derive the modified two *k*-ε equations model, and its constants. These constants were the topic of strict criticism such as that presented by Nagano and Itazu [37]. They have proved that all the constants in this model are invalid. Further research by Nagano and Itazu has highlighted other erroneous aspects of the RNG/*k*-ε model, such as the use of the ε-expansion technique [38]. They have also proved that the model is based on scale removal procedure rather than a Renormalization Group theory. This was also supported by the findings of Eyink [39]. Several fundamental errors of the RNG/*k*-ε model were also reported by more than a few careful mathematical discussions. The most rigorous of these discussions have been proposed by Teodorovich [40], Sukoriansky [41] and Wang and Wu [42].

Nevertheless, the RNG/*k*-ε model was reported to be successful in modeling different configurations of vortex/swirling flow. In the matter of fact, virtually all of the successful simulations with the RNG/*k*-ε model for vortex flows are reported by researchers who utilize the FLUENT® CFD solver [43–52]. In these simulations, two reasons were given for such prevalence of the RNG/*k*-ε model. The first is the swirl modification proposed by FLUENT® Inc. for their commercial solver, which is a software advantageous modification of the turbulent viscosity equation. The essence of such modification is based on empirical correlations which are not revealed to users. The second reason is a new additional production of dissipation term in the ε equation. The new term, R_ε, can be written in the following form:

$$R_\varepsilon = 2\nu_0 S_{ij} \overline{\frac{\partial u_l}{\partial x_i}\frac{\partial u_l}{\partial x_j}}. \tag{3}$$

In order to solve the ε equation, the R_ε term had to be evaluated. It was shown that such closure cannot be achieved using the methods based on ε expansion procedure, as described in [36]. Yakhot and Smith [53] postulated an expression for R_ε based on the additional expansion parameter η which is the ratio of the turbulent to mean strain time scale. The resulting expression is:

$$R_\varepsilon = \frac{\nu_T S^3 (1-\eta/\eta_0)}{1+\beta\eta^3} \tag{4}$$

Where $\eta = S\,\bar{k}/\bar{\varepsilon}$, $S = (2S_{ij}S_{ij})^{1/2}$, and $\eta_0 \approx 4.38$.

The constant β was chosen such as $\beta = 0.012$ which results in a value for the Von Karman constant of 0.4; a recommended value for turbulent channel flows. The R_ε/k-ε turbulence model presented by the authors adopted the R_ε term in the standard k-ε formulation. The transport equations of the R_ε/k-ε turbulence model can be expressed as [21]:

Equation for the turbulence kinetic energy (k):

$$\rho U_j \frac{\partial k}{\partial x_j} = \tau_{ij}\frac{\partial U_i}{\partial x_i} - \rho\varepsilon + \frac{\partial}{\partial x_j}\left[\left(\mu + \frac{\mu_T}{\sigma_k}\right)\frac{\partial k}{\partial x_j}\right] \quad (5)$$

where U_i is the mean velocity, x_i is the position vector, τ_{ij} is the Reynolds stress, μ_T is the eddy viscosity, σ_k is a closure coefficient that has a unity value, and ε is the dissipation rate.

Equation for the dissipation rate of turbulence kinetic energy (ε):

$$\rho U_j \frac{\partial \varepsilon}{\partial x_j} = C_{\varepsilon 1}\frac{\varepsilon}{k}\tau_{ij}\frac{\partial U_i}{\partial x_j} - C_{\varepsilon 2}\rho\frac{\varepsilon^2}{k} + \frac{\partial}{\partial x_j}\left[\left(\mu + \frac{\mu_T}{\sigma_\varepsilon}\right)\frac{\partial \varepsilon}{\partial x_j}\right] - \frac{\nu_T S^3(1-\eta/\eta_0)}{1+\beta\eta^3} \quad (6)$$

The eddy viscosity is expressed as $\mu_T = \rho C_\mu \dfrac{k^2}{\varepsilon}$ (7)

The model constants $C_{\varepsilon 1}$, $C_{\varepsilon 2}$, C_μ and σ_ε values are 1.44, 1.92, 0.09 and 1.3, respectively, as reported in [54,55].

4. Numerical procedures

4.1. Spatial discretization

A two dimensional, finite volume solver [56,57] was used to discretize the 2D flow domain through a first-order order upwind scheme. Several quadrilateral grids were generated for the purpose of ensuring that the solution is grid-independent, as detailed in Section 5. The SIMPLE algorithm was used to achieve the mass conservation between the pressure and velocity terms in the discretized momentum equation. Because the pressure variation between the discretized grid cells was expected to be irregular, a pressure staggering scheme [58] was used to interpolate the pressure values at the cell faces.

4.2. Operating and boundary conditions

The operating pressure and temperature were set to 1.013 bar and 290 K, respectively. These operating conditions were applied to the inlet air to calculate the density and viscosity, which was assumed to remain constant along the flow domain. Air was computationally supplied to the flow domain with a constant velocity and fully developed velocity profile. The pressure at the outlet section of the flow domain was constrained to the ambient pressure. Heat transfer due to viscous shear within the flow domain, and due to convection from the flow domain to ambient environment were both neglected. The Reynolds number of the flow inside the cavity was calculated based on the inlet velocity and cavity diameter as:

$$\mathrm{Re} = \frac{\rho U_{in} D}{\mu} \quad (8)$$

where U_{in} is the inlet velocity to the domain, D is the cavity diameter and ν is the kinematics viscosity of air. Since the diameter of cavity is held constant in the present analysis, the Reynolds number was varied according to the inlet velocity solely. Four different values of Reynolds number were examined in comparison with the LDA measurements of [19]. The values of the Reynolds number worked in the present study, and their corresponding inlet velocities are detailed in Table 1.

Table 1
Values of Reynolds number and corresponding inlet velocity for the present analysis.

Re	5.285×10^4	9.155×10^4	1.191×10^5	1.302×10^5
U_{in}	5.60	9.70	12.62	13.80

Table 2
Details of the four grids used in the grid independency study.

Grid	Number of grid cells	Minimum cell area (m^2)	Maximum cell area (m^2)
G1	9190	4.57×10^{-6}	2.80×10^{-5}
G2	16,169	2.76×10^{-6}	1.87×10^{-5}
G3	36,796	1.16×10^{-6}	8.44×10^{-6}
G4	93,341	4.9×10^{-7}	3.27×10^{-6}
G5	145,466	8.8410^{-8}	3.22×10^{-6}

5. Grid independency study

The solution was ensured to be independent from the grid quality and cell size by performing a grid independency study on four different grids. The convergence criteria was reached when the residuals was reduced four orders of magnitude. The details of the four grids, which were all of the hexahedral structure, are given in Table 2. The velocity and pressure profiles on line DE for the four computations are shown in Fig. 2. The grid independency computations were performed at $\mathrm{Re} = 9.876\times10^4$.

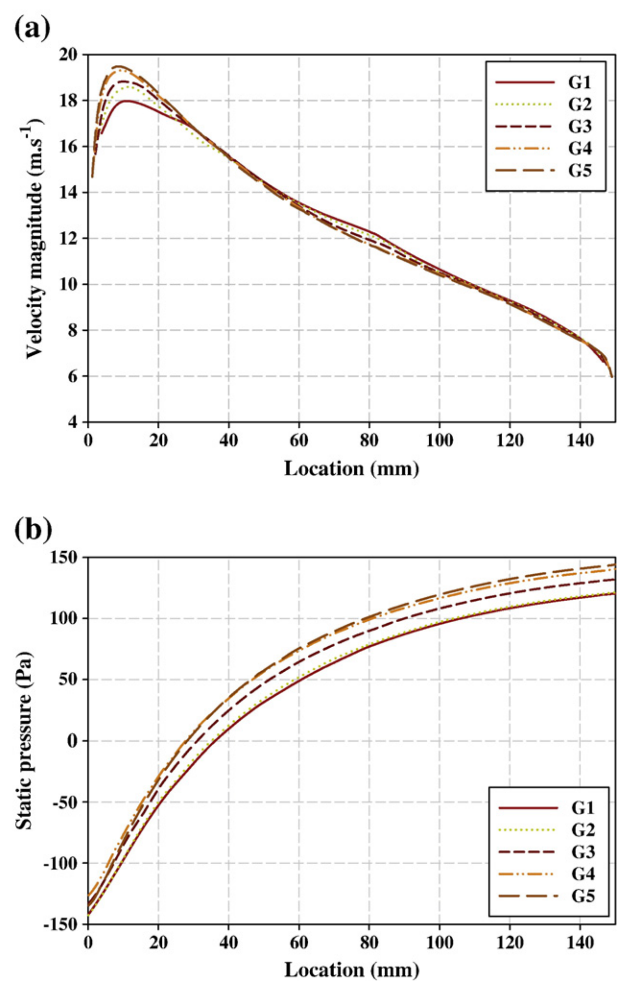

Fig. 2. Line (DE) grid-independency profiles of (a) velocity and (b) static pressure.

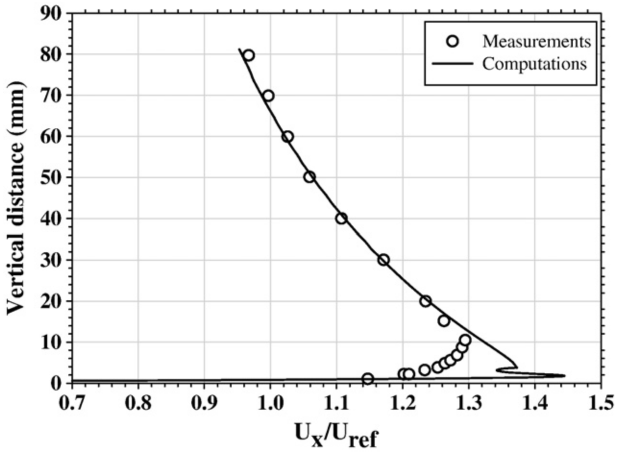

Fig. 3. Normalized computed X velocity component in comparison with measurements.

The grid independency study reveals rather slight differences between the five grids. There is approximately no difference between the velocity and pressure profiles predicted by G4 and G5. Thus, in order to optimize the computations for resources and quality, the grid G4 was adopted for the study.

6. Results and discussion

6.1. Flow separation at the cavity tip

The separated flow at the cavity tip (i.e. at point B) is indicated in Figs. 3 and 4 by the normalized velocity components in X and Y directions, respectively, in comparison with measurements at Re = 9.876×10^4. The predicted velocity in the X direction, U_X, is in a very good agreement with measurements. However, in the near-wall region, the velocity seems to have some disagreement with measurement. The maximum deviation of the predictions from the measured values at such region is in the order of 34% of the inlet velocity value. This disagreement in the near-wall region is attributed to the near-wall treatment of the geometry.

In Fig. 4, the predicted velocity in the Y direction has better agreement with measurements near to the wall. The location where the computations have the maximum disagreement with measurements is at a vertical distance of 20 mm, where the disagreement is up to 3.8% of the inlet velocity value.

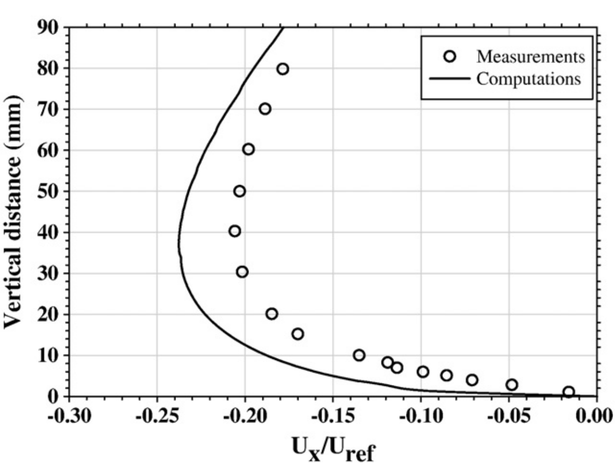

Fig. 4. Normalized computed Y velocity component in comparison with measurements.

6.2. The cavity flow

The basic intuition of the shear driven flow inside the cavity implies that such flow should exhibit a vortical shape. Several aspects of such flow were demonstrated and discussed experimentally in the original article [19]. It was reported, in such article, that the flow inside the cavity is a complete vortex flow with a core that has very small values of

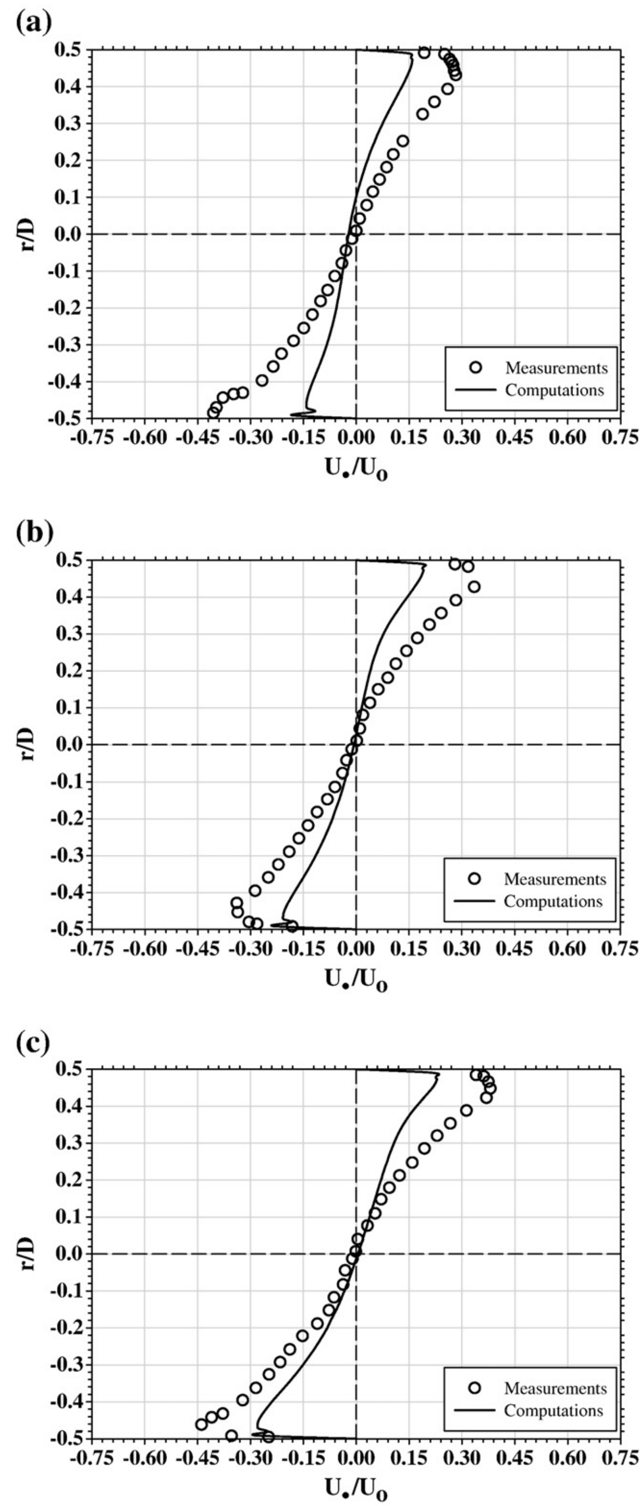

Fig. 5. Comparison between measured [19] and computed normalized tangential velocity along line BC in the cavity for (a) Re = 5.285×10^4 (b) Re = 9.155×10^4 and (c) Re = 1.302×10^5.

turbulence quantities. The core was suspected to be laminar or exhibiting minimized unsteadiness that produce the measured levels of turbulence. The focus of the present section, however, is to show that the modified turbulence model has successfully captured the main features of the vortex flow in the cavity.

As depicted in Fig. 5(a–c), the $R_\varepsilon/k\text{-}\varepsilon$ turbulence model provided predictions that agree with measurements qualitatively. At all examined Re values, the modified model successfully predicted the vortex motion in the cavity which is evident when observing the altering profile of normalized tangential velocity in Fig. 5. However, there is some quantitative difference between the predicted and measured values. The model underpredicts the tangential velocity in the cavity. When the Re number increases the quantitative deviation of the predictions from the measurement is reduced, as revealed by comparing the three Re values in Fig. 5.

7. Conclusion

Numerical computations of the shear driven vortex flow in a cylindrical cavity were performed using the recently proposed $R_\varepsilon/k\text{-}\varepsilon$ turbulence model. A review of the eddy viscosity turbulence models used for computing vortex flows was presented to justify the formulation of the modified model. The results of the computations were compared to recently published LDA measurements for the case, and the model demonstrated good agreement with such measurements at different values of Reynolds number. Such agreement included the predictions of the velocity over the separation point and inside the cavity. It was shown that the shear-driven vortex flow inside the cavity was successfully predicted. Future work should focus on the fine tuning of the model constants to achieve enhanced quantitative predictions and faster solution convergence. Some special formulation of the near-wall treatment in vortex flows has to be proposed for the model as well.

References

[1] R.D. Mills, On the closed motion of a fluid in a square cavity, Journal of the Royal Aeronautical Society 69 (1965) 116–120.
[2] F. Talebi, A.H. Mahmoudi, M. Shahi, Numerical study of mixed convection flows in a square lid-driven cavity utilizing nanofluid, International Communications in Heat and Mass Transfer 37 (1) (2010) 79–90.
[3] Y. Guo, R. Bennacer, S. Shen, D.E. Ameziani, M. Bouzidi, Simulation of mixed convection in slender rectangular cavity with lattice Boltzmann method, International Journal of Numerical Methods for Heat and Fluid Flow 20 (1) (2010) 130–148.
[4] C.J. Ho, F.H. Lin, Numerical simulation of three-dimensional incompressible flow by a new formulation, International Journal for Numerical Methods in Fluids 23 (10) (1996) 1073–1084.
[5] J.J. Wei, B. Yu, W.Q. Tao, Y. Kawaguchi, H.S. Wang, A new high-order-accurate and bounded scheme for incompressible flow, Numerical Heat Transfer, Part B: Fundamentals 43 (1) (2003) 19–41.
[6] M.M. Gupta, J.C. Kalita, New paradigm continued: further computations with streamfunction-velocity formulations for solving Navier–Stokes equations, Communications in Applied Analysis 10 (4) (2006) 461–490.
[7] A.A. Mohamad, R. Viskanta, Application of Low Reynolds Number k-ε turbulence model to buoyant and mixed flows in a shallow cavity, 1992.
[8] W.H. Yan, C.X. Zhang, N.N. Chen, G. Gao, Numerical simulation high Reynolds number lid-driven cavity flow using Gao-Yong turbulence equations, Shuikexue Jinzhan/Advances in Water Science 19 (3) (2008) 428–433.
[9] R.W.C.P. Verstappen, A.E.P. Veldman, Direct numerical simulation of turbulence at lower costs, Journal of Engineering Mathematics 32 (2–3) (1997) 143–159.
[10] A.V. Bunyakin, S.I. Chernyshenko, G.Y. Stepanov, High-Reynolds-number Batchelor-model asymptotics of a flow past an aerofoil with a vortex trappen in a cavity, Journal of Fluid Mechanics 358 (1998) 238–297.
[11] J.R. Koseff, H. Rhee, R.L. Street, Mixing in a stratified recirculating flow, 1983.
[12] N. Alleborn, H. Raszillier, F. Durst, Lid-driven cavity with heat and mass transport, International Journal of Heat and Mass Transfer 42 (5) (1999) 833–853.
[13] S.A. Isaev, P.A. Baranov, A.G. Sudakov, N.A. Mordynsky, Numerical analysis of vortex dynamics and unsteady turbulent heat transfer in lid-driven square cavity, Thermophysics and Aeromechanics 15 (3) (2008) 463–475.
[14] M. Cheng, K.C. Hung, Vortex structure of steady flow in a rectangular cavity, Computers and Fluids 35 (10) (2006) 1046–1062.
[15] S.A. Isaev, S.V. Guvernyuk, M.A. Zubin, Y. Prigorodov, Numerical and physical modeling of a low-velocity air flow in a channel with a circular vortex cell, Journal of Engineering Physics and Thermophysics 73 (2) (2000) 337–344.
[16] P.A. Baranov, S.V. Guvernyuk, M.A. Zubin, S.A. Isaev, Numerical and physical modelling of the circulation flow in a vortex cell in the wall of a rectilinear channel, Fluid Dynamics 35 (5) (2000) 663–673.
[17] C.-H. Bruneau, M. Saad, The 2D lid-driven cavity problem revisited, Computers & Fluids 35 (3) (2006) 326–348.
[18] H. Mercan, K. Atalik, Vortex formation in lid-driven arc-shape cavity flows at high Reynolds numbers, European Journal of Mechanics, B/Fluids 28 (1) (2009) 61–71.
[19] R. Savelsberg, I.P. Castro, Vortex flows in open cylinderical-section cavities, Experiments in Fluids 46 (2009) 485–497.
[20] A. Hokpunna, M. Manhart, A large-eddy simulation of vortex cell flow with incoming turbulent boundary layer, International Journal of Mechanical Systems Science and Engineering 1 (2007) 123–128.
[21] K.M. Saqr, H.S. Aly, M.A. Wahid, M.M. Sies, Numerical simulation of confined vortex flow using a modified k-ε turbulence model, CFD Letters 1 (2) (2009) 87–94.
[22] D.C. Wilcox, Turbulence modeling for CFD, DCW Inc., 1994.
[23] A.S. Almgren, J.B. Bell, C.A. Rendleman, M. Zingale, Low mach number modeling of type Ia supernovae. I. Hydrodynamics, The Astrophysical Journal 637 (2) (2006) 922–936.
[24] Y.A. Eldrainy, K.M. Saqr, H.S. Aly, M.N.M. Jaafar, CFD insight of the flow dynamics in a novel swirler for gas turbine combustors, International Communications in Heat and Mass Transfer 36 (9) (2009) 936–941.
[25] K.R. Menzies, An evaluation of turbulence models for the isothermal flow in a gas turbine combustion system, in: W. Rodi (Ed.), 6th International Symposium on Engineering Turbulence Modeling and Experiments, 2005, Sardinia, Italy.
[26] G. Hsiao, H. Mongia, Swirl cup modeling part III: grid independent solution with different turbulence models, 41th Aerospace Sciences Meeting & Exhibit, AIAA, Reno, Nevada, 2003.
[27] A. Smirnov, A. Lipatnikov, J. Chomiak, Simulations of swirl-stabilized premixed combustion, American Society of Mechanical Engineers, Pressure Vessels and Piping Division (Publication) PVP, ASME, San Diego, CA, USA, 1998.
[28] S.J. Tarr, G. Allen, A. Aroussi, S.J. Pickering, Interaction of swirling flows from two adjacent coal burners, American Society of Mechanical Engineers, Fluids Engineering Division (Publication) FED, ASME, Vancouver, Can, 1997.
[29] Y.P. Li, Q. Zhang, F. Gu, Y.Q. Xu, Numerical study on the effect of reverse swirl of secondary air on flue gas imbalance in large tangentially fired boiler, Zhongguo Dianji Gongcheng Xuebao/Proceedings of the Chinese Society of Electrical Engineering 21 (9) (2001) 33–37.
[30] U. Engdar, J. Klingmann, Investigation of two-equation turbulence models applied to a confined axis-symmetric swirling flow, American Society of Mechanical Engineers, Pressure Vessels and Piping Division (Publication) PVP, 2002 Vancouver, BC.
[31] M.R. Halder, S.K. Som, Numerical and experimental study on cylindrical swirl atomizers, Atomization and Sprays 16 (2) (2006) 223–236.
[32] Y.A. Eldrainy, H.S. Aly, K.M. Saqr, M.N.M. Jaafar, A multiple inlet swirler for gas turbine combustors, International Journal of Mechanical Systems Science and Engineering 2 (2) (2010) 106–109.
[33] K.M. Saqr, M.M. Sies, H.S. Aly, M.A. Wahid, Characteristics of turbulent whirling flow in an asymmetric passage, Proceedings of the 2nd International Meeting on Advances in Thermo-Fluids (IMAT), Universiti Indonesia, Taman Safari, Indonesia, 2009, pp. 97–101.
[34] F.M. Erdal, S.A. Shirazi, Local velocity measurements and computational fluid dynamics (CFD) simulations of swirling flow in a cylindrical cyclone separator, Journal of Energy Resources Technology, Transactions of the ASME 126 (4) (2004) 326–333.
[35] V. Yakhot, S.A. Orszag, Renormalization-group analysis of turbulence, Physical Review Letters 57 (14) (1986) 1722–1724.
[36] V. Yakhot, S.A. Orszag, Renormalization group analysis of turbulence. I. Basic theory, Journal of Scientific Computing 1 (1) (1986) 3–51.
[37] Y. Nagano, Y. Itazu, Renormalization group theory for turbulence: assessment of the Yakhot–Orszag–Smith theory, Fluid Dynamics Research 20 (1–6) (1997) 157–172.
[38] Y. Nagano, Y. Itazu, Renormalization group theory for turbulence: eddy-viscosity type model based on an iterative averaging method, Physics of Fluids 9 (1) (1997) 143–153.
[39] G.L. Eyink, The renormalization group method in statistical hydrodynamics, Physics of Fluids 6 (1994) 3063–3078.
[40] E.V. Teodorovich, On the Yakhot–Orszag theory of turbulence, Fluid Dynamics 29 (6) (1995) 770–779.
[41] S. Sukoriansky, B. Galperin, I. Staroselsky, Cross-term and ε-expansion in RNG theory of turbulence, Fluid Dynamics Research 33 (4) (2003) 319–331.
[42] X.H. Wang, F. Wu, One modification to the Yakhot–Orszag calculation in the renormalization-group theory of turbulence, Physical Review E 48 (1) (1993).
[43] A. Secchiaroli, R. Ricci, S. Montelpare, V. D'Alessandro, Numerical simulation of turbulent flow in a Ranque–Hilsch vortex tube, International Journal of Heat and Mass Transfer 52 (23–24) (2009) 5496–5511.
[44] F. Kaya, I. Karagoz, Performance analysis of numerical schemes in highly swirling turbulent flows in cyclones, Current Science 94 (10) (2008) 1273–1278.
[45] K.S. Reddy, D.N. Reddy, C.M. Varaprasad, Experimental and numerical investigations of swirling flows in a reverse flow gas turbine combustor, Collection of Technical Papers - 37th AIAA Fluid Dynamics Conference, 2007 Miami, FL.
[46] I. Karagoz, F. Kaya, CFD investigation of the flow and heat transfer characteristics in a tangential inlet cyclone, International Communications in Heat and Mass Transfer 34 (9–10) (2007) 1119–1126.

[47] A. Escue, J. Cui, Numerical investigation of swirling pipe flows, American Society of Mechanical Engineers, Fluids Engineering Division (Publication) FED, 2006 Chicago, IL.
[48] L. Huang, K. Kumar, A.S. Mujumdar, Simulation of a spray dryer fitted with a rotary disk atomizer using a three-dimensional computional fluid dynamic model, Drying Technology 22 (6) (2004) 1489–1515.
[49] A. Aroussi, S. Kucukgokoglan, S.J. Pickering, M. Menacer, Evaluation of three turbulence models in isothermal swirling flows from four adjacent burners, Proceedings of the ASME Fluids Engineering Division Summer Meeting, 2003 New Orleans, LA.
[50] B. Zhou, B.A. Fleck, F. Bouak, J.E.D. Gauthier, Comparison of swirling effects on ejector performance using four turbulence models, Canadian Aeronautics and Space Journal 46 (4) (2000) 178–182.
[51] A. Gupta, R. Kumar, Three-dimensional turbulent swirling flow in a cylinder: experiments and computations, International Journal of Heat and Fluid Flow 28 (2007) 249–261.
[52] A.M. Jawarneh, H. Tlilan, A. Al-Shyyab, A. Ababneh, Strongly swirling flows in a cylindrical separator, Minerals Engineering 21 (5) (2008) 366–372.
[53] V. Yakhot, L.M. Smith, The renormalization group, the e{open}-expansion and derivation of turbulence models, Journal of Scientific Computing 7 (1) (1992) 35–61.
[54] B.E. Launder, D.B. Spalding, Lectures in Mathematical Models of Turbulence, Academic Press, London, England, 1972.
[55] B.E. Launder, D.B. Spalding, The numerical computation of turbulent flows, Computer Methods in Applied Mechanics and Engineering 3 (1974) 269–289.
[56] K.M. Saqr, H.S. Aly, M.M. Sies, M.A. Wahid, Effect of Free Stream Turbulence on NO_x and Soot Formation in Turbulent Diffusion CH_4-Air Flames, International Communications on Heat and Mass Transfer 37 (6) (2010) 611–617.
[57] K.M. Saqr, M.M. Sies, M.A. Wahid, Numerical investigation of the turbulence-combustion interaction in non-premixed CH_4/Air Flames, International Journal of Applied Mathematics and Mechanics 5 (8) (2009) 69–79.
[58] S.V. Patankar, Numerical Heat Transfer and Fluid Flow, Series on Computational Methods in Mechanics and Thermal Science, Taylor & Francis, Washington, DC, 1980.